

# Carbon Based Coatings for Thermal Detectors: Laser Damage and Thermal Efficiency

Krishna Ramadurai<sup>a</sup>, Laurence Lewis<sup>b</sup>, Chris Cromer<sup>b</sup>, Roop L. Mahajan<sup>c</sup>, Katherine E. Hurst<sup>b</sup>, and John H. Lehman<sup>\*b</sup>

<sup>a</sup>Department of Mechanical Engineering, University of Colorado, 1111 Engineering Drive  
Boulder, CO 80309-0427

<sup>b</sup>National Institute of Standards and Technology, 325 Broadway, Boulder, CO 80305

<sup>c</sup>ICTAS (Institute for Critical Technologies and Applied Science), Virginia Polytechnic Institute and State University, 1880 Pratt Drive, Suite 2000 (0493), Blacksburg, VA 24061

## ABSTRACT

The laser damage threshold and absorption efficiency of a variety of carbon based thermal coatings for laser power and energy measurements have been investigated. Carbon based paint, carbon fibers, as well as single wall carbon nanotubes (SWCNTs) and multiwalled carbon nanotubes (MWCNTs), were applied to a water cooled copper substrate. The heating of the water was measured to determine power absorbed by the sample during laser exposure. Before and after exposure to 10.6  $\mu\text{m}$  laser radiation, optical and electron microscopy as well as Raman spectroscopy were employed to evaluate the coating topology and composition. These early measurement results demonstrate that a MWCNT coating has a damage threshold of approximately 1686  $\text{W}/\text{cm}^2$ , which is four times as large as that measured for SWCNTs and fifteen times greater than that of carbon based paint.

Keywords: carbon nanotubes, laser damage, Raman spectroscopy, thermal detector

## 1. INTRODUCTION

During the last 50 to 100 years, thermal detector coatings based on carbon-based paints, diffuse metals (gold black, silver black), oxidized metals (anodized aluminum) and other materials have been investigated with regard to spectral uniformity and resistance to damage and aging. In principle, the spectral responsivity of a thermal detector depends on the variation of reflectance of the detector coating as a function of wavelength. Betts et al.<sup>1</sup> studied the infrared reflectance properties of three metal blacks (platinum, aluminum and nickel) and two black paints. It was shown that the platinum black provided the best performance, with consistently low reflectance up to a wavelength of at least 12  $\mu\text{m}$ . Advena et al.<sup>2</sup> described a process to produce gold black films with high absorptance in the far infrared for wavelengths as long as 50  $\mu\text{m}$ . Nelms and Dowson<sup>3</sup> demonstrated a repeatable process to produce gold black coatings with absorption over 90 % out to wavelengths beyond 40  $\mu\text{m}$ . Such coatings, however, are vulnerable to damage at high optical powers from forced air, as well as aging and hardening at UV wavelengths<sup>4</sup>. Lehman et al.<sup>5</sup> deposited gold black coatings on thin, freestanding pyroelectric detector substrates and determined the damage threshold to be 38  $\text{mJ}/\text{cm}^2$  upon exposure to a 193 nm wavelength excimer laser.

Carbon nanotubes (CNTs), with exceptional mechanical strength and thermal conductivity, serve as ideal candidates for detector coatings. Lehman et al.<sup>6</sup> also studied the spatial and directional uniformity of SWCNTs as a thermal-absorption coating on a large area pyroelectric detector using a diode laser operating at a wavelength of 0.85  $\mu\text{m}$ . The spatial and directional uniformity measurement results, which indicated variations of approximately 1 %, were favorable compared

\* [lehman@boulder.nist.gov](mailto:lehman@boulder.nist.gov); phone 1-303-497-3654

Contribution of the US government, not subjected to copyright

with other alternatives. Damage threshold and thermal conductivity comparisons with black paint demonstrated the promise of CNTs as detector coatings. More recently, Theocharous et al.<sup>7</sup> evaluated the performance of a pyroelectric detector with a MWCNT coating in the 0.9-14  $\mu\text{m}$  wavelength range. The relative spectral responsivity of this detector was shown to be flat over most of the wavelength range examined, and the spectral flatness was shown to be comparable to the best IR black coatings currently available. The CNT coatings were reported to be much more durable than other IR black coatings, such as metal blacks, which are commonly used to coat thermal detectors in the IR region.

## 2. EXPERIMENTAL DETAILS

### 2.1. Coating preparation

In the present study, we evaluated the damage threshold of MWCNT and SWCNT coatings applied using a simple airbrush technique and provide a comparison with carbon based paint and carbon fibers with incident heat fluxes upto  $10 \text{ kW/cm}^2$  using a 2 kW  $\text{CO}_2$  laser at a wavelength of  $10.6 \mu\text{m}$ . Based on the performance of the coatings, scanning electron microscopy (SEM) and Raman microscopy were also employed to characterize the MWCNT samples. Commercially obtained MWCNTs and SWCNTs were used to develop the coatings. The nanotubes (10 % by weight) were dispersed in a solution of chloroform and the mixture was sonicated for a period of 10 minutes. The nanotubes mixture was then sprayed (using an airbrush) onto a polished copper substrate ( $62 \text{ mm} \times 24 \text{ mm} \times 0.8 \text{ mm}$ ) to produce samples for damage testing. In addition to the CNT samples, a commercial diffuse black paint and a sample with graphite fibers grown by chemical vapor deposition (CVD) were also tested.

### 2.2. Damage testing

Fig. 1 depicts the experimental setup used to evaluate the damage threshold of the sample coatings.

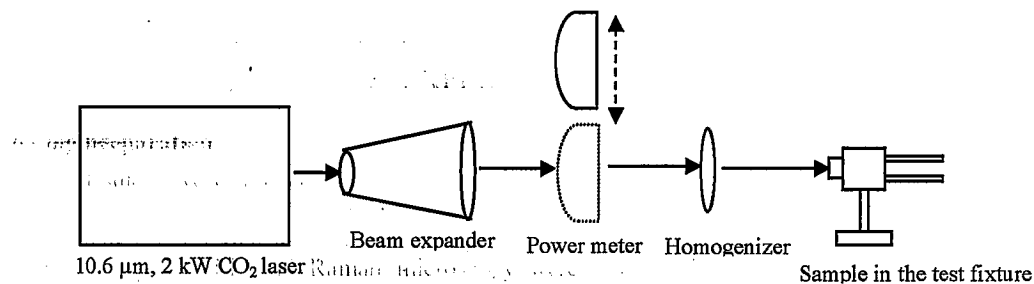


Fig. 1. Schematic of test setup to study coating damage upon laser incidence

A 2 kW  $\text{CO}_2$  laser operating at a wavelength of  $10.6 \mu\text{m}$  and capable of a power density of  $10 \text{ kW/cm}^2$  was used as the source for local heating and eventual damage. The laser passed through a beam expander and then a faceted ZnSe lens that acted as a homogenizer of the beam intensity. This resulted in a  $0.54 \text{ cm}$  square beam at the point of incidence on the sample. The sample was mounted in a test fixture that also has provision for cooling water to flow behind the sample to remove the heat generated due to the incidence of the laser radiation. A plastic mesh was placed between the water and the copper sample to induce turbulence to enhance thermal exchange. The power,  $P_A$ , absorbed by the sample was calculated as

$$P_A = \rho_W C_W \Delta T \quad (1)$$

where  $\rho_W$  refers to the mass flow rate of the water (set at  $\sim 0.0667 \text{ kg}\cdot\text{sec}^{-1}$ ),  $C_W$  is the specific heat capacity of water ( $4181.3 \text{ J}\cdot\text{kg}^{-1}\cdot\text{K}^{-1}$  at  $298 \text{ K}$ ), and  $\Delta T$  is the difference (K) between the input temperature and spatially averaged output temperature of the cooling water as acquired from thermistors located upstream and downstream, respectively. The absorption efficiency,  $\eta$ , of the coating was calculated as

$$\eta = \frac{P_A}{P_I}, \quad (2)$$

where the incident laser power,  $P_I$ , was measured with a NIST calibrated commercially available thermopile. The magnitude of  $\eta$  was evaluated for incremental laser power input. The damage threshold was defined at the laser input power where  $\eta$  was significantly decreased. That is, for successive increments of increasing power the value of  $\eta$  was less than the previous increment. In the present context, damage threshold could also be defined as the incident power  $P_I$  which is characterized by a visual damage to the coating. At the damage threshold, there is an apparent decrease in  $P_A$  due to coating damage. It is to be noted that the power density where visual damage is observed is lower than the power density where the absorption efficiency changes. Sample characterization was performed after incidence at the power density where the drop in  $\eta$  was significant. After each damage test, the samples were visually inspected by use of an SEM and also quantitatively analyzed by visible Raman spectroscopy.

The uncertainty of the damage measurements has not been fully evaluated. The uncertainty of the measurement in the absorbed power with the cooling water is typically on the order of 1 %, based on knowledge of the mass flow rate, specific heat and temperature change of the flowing water. The thermopile is capable of measurements having an uncertainty of approximately 1.2 %<sup>3</sup>. In this study, the uncertainty of the measurement is likely dominated by the qualitative determination of the damage threshold, the beam nonuniformity, and the variability in the coating preparation due to variability in the material purity, coating thickness and topology of the nominal coating preparation. Repeated damage experiments on coating preparations that are considered to be nominally the same ranged in magnitude by  $\pm 15$  %. These variations are discussed in Section 3.

### 2.3. Visual damage qualification

Optical microscopy was employed in conjunction with SEM by use of a Low Vacuum Scanning Electron Microscope (LV-SEM) to visually study coating damage. The SEM was also equipped with Energy Dispersive X-ray (EDX) in order to study the composition of the unexposed and the exposed sample.

### 2.4. Raman spectroscopy

Raman spectroscopy measurements were performed in the backscattering configuration with 7 mW from an argon ion laser providing 488 nm (2.54 eV) excitation. A 55 mm telephoto lens was employed to both focus the beam to  $\sim 0.25$  mm<sup>2</sup> area and to collect the Raman scattered light. The scattered light was analyzed with a 0.27 m grating spectrometer equipped with a liquid nitrogen cooled charge coupled detector and a holographic notch filter. Information derived from the Raman spectroscopy is important in terms of characterizing the relative quantities of carbon impurities and defective sites on the MWCNTs.

## 3. RESULTS AND DISCUSSION

Table 1 provides measurements of the damage threshold and average absorption efficiency of the various coatings tested for irradiance with the 10.6  $\mu$ m laser. These values are reported based on observable damage to the coating. It can be seen that the carbon fiber sample had the lowest damage threshold. At lower levels of  $P_I$ , SEM images revealed the formation of sharp structures, suggesting that the heat from the laser had resulted in ablation of the layers. The sample also had high amorphous carbon content, which was verified independently through Transmission Electron Microscopy (TEM). The onset of damage occurred at a relatively moderate power level, resulting in a low damage threshold.

Table 1. Experimental evaluation of the damage threshold and average absorption efficiency of various coatings.

Coating	Damage Threshold ( $W/cm^2$ )	Average absorption efficiency (%)
Carbon fibers grown by CVD	46.5	76.5
Black paint	115.3	87.2
SWCNT coating	403.5	91.1
MWCNT coating	1686.5	83

The black paint sample demonstrated a relatively higher damage threshold and average absorption efficiency. However at higher power levels, cracking occurred, resulting in the exposure of the base copper, thereby reducing  $P_A$ . The sprayed SWCNT coating demonstrated a high damage threshold, as can be seen from Table 1 and the highest average absorption efficiency. However the damage threshold of MWCNT coating outperformed that of SWCNT coating and the carbon paint by a factor of four and fifteen times respectively, which could be in part to the presence of multiple walls that resisted the damage at higher  $P_I$  levels.

The samples were irradiated at intensities which were higher than the damage threshold to observe the effects on the various coatings. The laser power was increased to the point where a significant drop in the absorption efficiency was registered. Figs. 2(a) and (b) show optical images of the black paint sample and the MWCNT coating, respectively, after irradiation with the  $CO_2$  laser. Fig. 2(a) shows the irradiated black paint sample with cracks providing evidence of damage. In Fig. 2(b), the damaged region can be observed by the boundary between the dark region and the grid-like region of a different contrast (representative of the effect of the homogenizer lens grid).

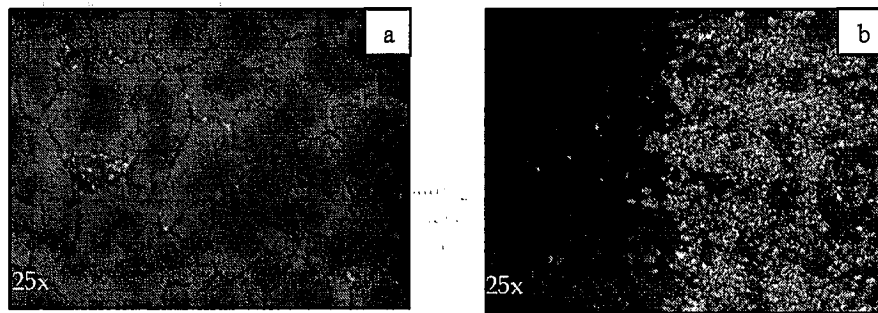


Fig. 2. Optical microscopy images of (a) MWCNT coating & (b) carbon based paint after laser irradiation at  $\sim 3000 W/cm^2$ .

SEM images of the MWCNT coating before and after the laser exposure at an intensity twice the damage threshold are presented in Fig. 3(a) and 3(b), respectively. EDX analysis indicated the white spots in Fig. 3(a) were representative of catalyst impurities in the nanotubes. Fig. 3(b) shows an SEM image of the same area after the irradiation with the laser, in which a reduction in the amount of impurities is observed.

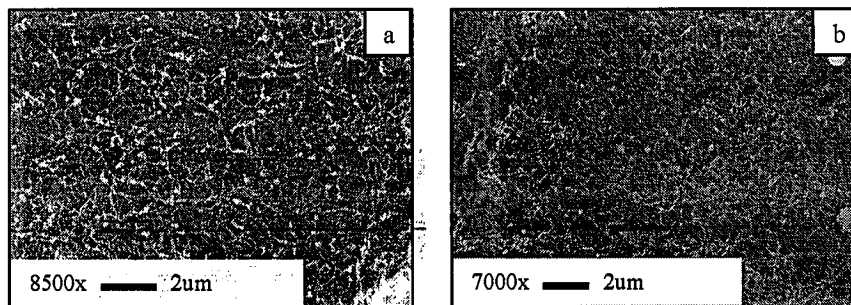


Fig. 3. SEM images of the MWCNT coating (a) before exposure and (b) after exposure at  $\sim 3000 W/cm^2$

Raman spectroscopy was employed to characterize the effect of laser damage on the MWCNT coating. Fig. 4 shows the Raman spectra normalized to the intensity of the G-band, before and after the material was exposed to an irradiation at  $\sim 3000 \text{ W/cm}^2$ . The "G band" at  $1500\text{-}1650 \text{ cm}^{-1}$  is a compilation of bands originating from the in-plane vibrational modes of carbon in the curved graphite lattice, while the "D-band" at  $\sim 1350 \text{ cm}^{-1}$  is generated by symmetry lowering effects such as defects, tube ends or the presence of non-nanotube carbon impurities<sup>9</sup>. A broad D-band is characteristic of the presence of non-nanotube carbon impurities such as amorphous carbon or the presence of nanocrystalline graphite<sup>10</sup>. The full-width-at-half-maximum (FWHM) of the D-band, listed in Fig. 4, decreases from 43.61 to 38.40 and is therefore consistent with the removal of carbon impurities from the MWCNT sample.

The D-band/G-band intensity ratio (D/G) provides a relative measure of the amount of defects and the degree of graphitization in the MWCNT sample and the degree of graphitization<sup>9</sup>. The D/G ratio for the spectra in Fig. 4 increases from 0.600 to 0.741 after being exposed to the laser. This indicates an increase in the number of defects in the sample and that the MWCNTs are damaged by irradiation at these conditions. Raman analysis of the samples before and after laser irradiation at  $\sim 3000 \text{ W/cm}^2$  indicates that although carbon impurities are removed from the sample, defects are also created in the MWCNTs.

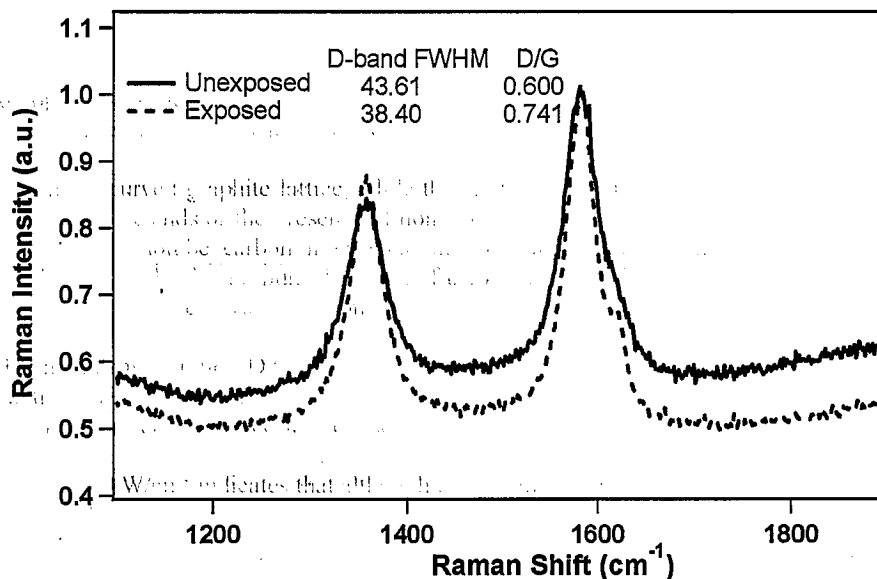


Fig. 4. Raman spectra taken at 488 nm excitation for a MWCNT coating before and after exposure to  $\sim 3000 \text{ W/cm}^2$

The onset of damage to the coatings may be the result of several factors. Particularly, in a carbon nanotube based coating, where impurities such as catalyst particle remnants and amorphous carbon have an inevitable presence, the oxidation of such impurities will damage the coating at a lower temperature. Also, the beam profile incident on the sample is not completely uniform, so higher intensity regions of the beam may damage surface layers. In addition, increased laser power fluctuations from operation of the high power laser at its low power limit may also result in the same surface layer damaging effect. Recent investigations have given valuable insights into the effects of transferring large amounts of kinetic energy from laser radiation to a carbon nanotube lattice<sup>11</sup>. Ma et al.<sup>12</sup> found that the structure changes induced in nanotubes caused by laser irradiation was strongly dependent on the initial laser parameters. Sintering of several tubes together was seen at lower power densities, and the restructuring of nanotubes into more energetically favorable and stable carbon nanoparticles occurred at high power densities. In addition, after enough energy was absorbed by the tubes, a high defect density in the structure of the tubes became apparent. Because of the morphology changes of CNTs under irradiation, an investigation of multi-exposures per site to thermally anneal the defects may prove a worthy course for further investigation.

The damage threshold based on visual damage to the coating is characterized by a relatively higher value of  $\eta$  and a noticeable decrease in the thickness of the coating. However, the threshold is lower than the value at which  $\eta$  was significantly decreased, which could be attributed to the presence of a thin layer of the nanotubes possibly undergoing structural changes and thereby accommodating higher power densities. The damage threshold demonstrated by the MWCNT coating was higher than the other samples tested, but the average absorption efficiency was lower than that of the SWCNT coating and carbon paint. Theocharous et al.<sup>7</sup> evaluated the spectral responsivity of MWCNT coating on pyroelectric detector in the IR region and demonstrated the spatial uniformity of the profile. The relative spectral responsivity of this detector was shown to be spectrally invariant over most of the wavelength range examined and was shown to be comparable (in terms of spectral neutrality) to the best IR black coatings currently available. This result is promising because black coatings with spectrally flat absorbance profiles are usually associated with the highest absorbance values<sup>3</sup>. This evidence serves to demonstrate the fact that MWCNT coatings have a future prospect for thermal detector coatings by virtue of their high damage threshold and flat spectral response over a wide wavelength range.

#### 4. CONCLUSIONS

We have experimentally measured the damage threshold of MWCNT, SWCNT, carbon fiber coatings and provided a comparison with commercially used black paint. Optical microscopy and SEM were employed to visually study the effect of the laser irradiation. The airbrushed multiwalled nanotube coating with a damage threshold of 1686.5 W/cm<sup>2</sup> outperforms the airbrushed single-walled nanotube coating by a factor of four and the black paint by a factor of fifteen. Raman spectroscopy showed the effect of the laser irradiation on the MWCNT coating by the removal of amorphous carbon and catalyst impurities. The average absorption efficiency of MWCNTs was lower when compared to the carbon paint, but the flatness of the spectral responsivity, coupled with its high thermal conductivity, holds great promise in its applicability as a coating for thermal detectors.

#### 5. ACKNOWLEDGEMENTS

Thanks to Anne Dillon of The National Renewable Energy Laboratory for assistance with the Raman spectroscopy measurements.

#### 6. REFERENCES

1. D.B. Betts, F.J.J. Clarke, L.J. Cox, and J.A. Larkin, "Infrared reflection properties of 5 types of black coating for radiometric detectors," *J Phys. E Sci. Instrum.*, 18 (8), 689-696 (1985).
2. D. J. Advena, V. T. Bly, and J. T. Cox, "Deposition and characterization of far-infrared absorbing gold black films," *Appl. Opt.*, 32, 1136 - 1144. (1993).
3. N. Nelms and J. Dowson, "Goldblack coating for thermal infrared detectors," *Sensor Actuat. A-Phys.*, 120(2), 403-407 (2005).
4. J. Lehman and A.C. Dillon, "Carbon-nanotube coatings promise better thermal detectors," *Laser Focus World*, 41(7), 81-87 (2005).
5. J. Lehman, E. Theocharous, G. Eppeldauer, and C. Panell, "Gold-black coatings for freestanding pyroelectric detectors," *Meas. Sci. Technol.*, 14, 916-922 (2003).
6. J.H. Lehman, C. Engtrakul, T. Gennett, and A. C. Dillon, "Single-wall carbon nanotube coating on a pyroelectric detector," *Appl. Opt.*, 44(4), 483-488 (2005).
7. E. Theocharous, R. Deshpande, A.C. Dillon, and J. Lehman, "Evaluation of a pyroelectric detector with a carbon multiwalled nanotube black coating in the infrared," *Appl. Opt.*, 45(6), 1093-1097 (2006).
8. E.D. West and K.L. Churney, "Theory of Isoperibol Calorimetry for Laser Power and Energy Measurements" *J. Appl. Phys.*, 41, 2705 - 2712 (1970).
9. A. C. Dillon, A. H. Mahan, P. A. Parilla, J. L. Alleman, M. J. Heben, K. M. Jones, and K. E. H. Gilbert, "Continuous hot wire chemical vapor deposition of high-density carbon multiwall nanotubes," *NanoLett.*, 3, 1425-1429 (2003).

10. A.C. Dillon, M. Yudasaka, and M.S. Dresselhaus, "Employing Raman spectroscopy to qualitatively evaluate the purity of carbon single-wall nanotube materials", *J. Nanosci Nanotech.*, 4(7), 691-703 (2004).
11. P. Corio, P.S. Santos, M.A. Pimenta, and M.S. Dresselhaus, "Evolution of the molecular structure of metallic and semiconducting carbon nanotubes under laser irradiation," *Chem. Phys. Lett.*, 360, 557-564 (2002).
12. R.Z. Ma, B.Q. Wei, C.L. Xu, J. Liang, and D.H. Wu, "The morphology changes of carbon nanotube under laser irradiation" *Carbon*, 38, 623-641 (2000).

## Damage of thermal detector platforms based on metal-carbon nanotube composites [6403-74]

Q What kind of atmosphere were you using over the top of the samples in the coatings in the power meter?

A We just left them at in oxygen atmosphere, we didn't alter the atmosphere at all.

Q How easy is it to apply this carbon nanotube surface to a curved surface? If you had to do this kind of coating on a tube, would it be easy to do so?

A That is one of the limitations we have with the air brushing that the tube is on, is getting it into the complex geometries. It's been done because we airbrushed the paint on and that is able to airbrush the inside of the cone fairly easily so it can be expanded into more complex geometries.

Q Did you try any shorter wavelengths such as near-IR or visible? Do the damage thresholds remain similar in the absorption regions?

A Actually at NIST were using the most powerful laser we have, a 2 kilowatt CO2 laser at 10.6. We are doing testing now at a 01.06 micrometer wavelength using a Nd: YAG laser at near visible wavelengths.